Electronic Supplementary Material (ESI) for Lab on a Chip.

Supporting Information

Three-dimensional heterogeneous assembly of coded microgels using an untethered mobile micro-gripper

*Su Eun Chung†, Xiaoguang Dong†, and Metin Sitti**

† Equally contributing authors

Gripping characterization and analysis

To achieve the capability of picking-and-placing and assembling hydrogels in 3D, the grippers were designed to have proper beam deflecting ability to be able to pick, transport and release a hydrogel of a given size and shape. The gap distance between two gripping magnets of a gripper was designed to be slightly smaller than the hydrogel to be assembled. When the gripper was holding a hydrogel, the final gap distance between the gripping magnets or the total deflection of gripper beams were fixed as constants depending on the size of the hydrogel. The total deflection δ_{total} of one thin beam is a summation of two different deflections, the deflection δ_B by the magnetic torque T and the deflection δ_S by the reactive normal surface N of the hydrogel (Figure S1(b)) as $\delta_{total}=\delta_B+\delta_S$. Assuming a straight single beam with thickness t, width w, and length L, and neglecting any interaction between gripping magnets, the small deflection by magnetic torque is given as

$$\delta_B = \frac{TL^2}{2EI} \tag{1}$$

where E is the elastic modulus of the beam and $I = \frac{tw^3}{12}$ is the area moment of inertia of the rectangular beam cross-section. The magnetic torque is proportional to the applied magnetic field B and the magnetic moment m of the gripping magnets and the sine of the angle between the magnetic moment and the applied magnetic field. Assuming that the field is perpendicular to the gripper magnetization direction, the magnetic torque can be obtained by $T = mB$. Therefore, through substitution the gripper deflection by the magnetic torque can be expressed as

$$\delta_B = \frac{mL^2B}{2EI} \quad (2)$$

When the gripper was holding the hydrogel, the deflection of the gripper beam was also affected by the reactive normal surface force *N* of the hydrogel to the gripping magnets, which is given as

$$\delta_S = \frac{NL^3}{3EI} \quad (3)$$

Therefore, the total deflection for the one beam is

$$\delta_{total} = \frac{mL^2B}{2EI} + \frac{NL^3}{3EI} \quad (4)$$

which is kept constant because the final gap distance between the gripping magnets was fixed as the size of the handle of the hydrogel, and the total deflection of the gripper beam is linearly proportional to the final gap distance. The friction force f between the gripper tips and the hydrogel helps balancing the apparent weight (weight after considering the buoyant force) of the hydrogel W in 3D. It has two components induced by the adhesion and normal load, which can be summarized in the following equation under the assumption of a smooth and undamaged contact surface.[1]

$$f = \tau A + \mu N \quad (5)$$

where A is the real contact area between the gripper tip and the hydrogel which can be obtained by using a micro/nanoscale contact mechanics model after checking the dimensionless Tabor parameter[2]. The critical shear stress $\tau = \frac{G_1 G_2}{15(G_1 + G_2)}$ is dependent on the bulk shear modulus

$G_i = \frac{E_i}{2(1+v_i)}, i = 1,2$ where E_i is the elastic modulus of the contacted materials and v_i is the Poisson's ratio.

The gripping analysis here indicates that the capability of holding hydrogels of different weights depends on the provided maximum friction. The load-induced component can be changed by controlling the surface normal force N by programming the applied magnetic field or modifying the friction coefficient with different contact surface roughness. The gripper tips were designed to fit to the shape of the hydrogels for maximum contact area to increase adhesion-induced friction. In addition, the adhesion-induced component can also be controlled by changing the ratio of the PBS solution in water.

Based on the above analysis of gripping, the relationship between the maximum provided friction force and design parameters, such as beam length, beam width, and materials, was simulated as shown in Figure S2. The simulation results indicated large beam length and width and elastic modulus of the material were required to achieve a high friction force for better transportation ability. However, the minimum required magnetic field strength is also needed to be studied to ensure the gripper arm can be opened within the maximum allowed magnetic field of the electromagnetic system due to hardware limitation. The minimum magnetic fields to open the gripper for different beam length, width and elastic modulus of the material were shown in Figure S3, which indicated the minimum required magnetic field increased quickly with an increased beam length, width, or elastic modulus Therefore, only a proper range of design parameters could satisfy the requirements of both large friction for better grabbing and small magnetic field strength for easy opening. In our experiments, the beam length and width of the gripper were around 700 μm and 70 μm, respectively, with a relative error about 10% due to the fabrication error. The elastic modulus of the mixed material of magnetic particles, polyurethane and glass bead was 9.8 MPa.

Heterogeneous 3D assembly of hydrogels

Hydrogels with different shapes and colors were constructed to a variety of 3D geometries using an untethered magnetic micro-gripper. Figure S4 showed a robotic heterogeneous assembly of hydrogels on four different posts. Figure S4(a)-(e) showed selected frames from a video showing the robotic heterogeneous assembly of hydrogels on multiple posts. Top microscope images in Figure S4(a)-(e) showed top views (x-y plane) and bottom images showed side views (y-z plane) of the assembly process. During the whole assembly process, all the hydrogels were sequentially and individually manipulated to the target posts in a flexible order of stacks for assembly by tele-operated control. The schematic illustration in Figure S4(f) showed the constructed 3D structure composed of twelve different hydrogels on four posts. Corresponding SEM images in Figure S4(g)-(h) showed that different shape-coded hydrogels were heterogeneously assembled on four different posts. Figure S4(i)-(k) gave another two examples of complex heterogeneous 3D structures assembled on four different posts using the micro-gripper. In addition to the four posts assembly, Figure S5 showed scalable large complex 3D assembly on eight different posts constructed by the micro-gripper. Total fifteen and twenty-four hydrogels with seven different types were assembled on eight posts as shown in Figure S5(a)-(c) and (d)-(f), respectively.

Videos

Video S1. Gripping function and 3D motion

This video shows the zoomed-in process of grabbing hydrogel and zoomed-out 3D motion control by magnetic force levitation.

Video S2. Multi-layer assembly of hydrogels on a single post

This video shows multi-layer heterogeneous assembly of hydrogels on a single post. Ten hydrogels were assembled on a single post by simply repeating pick-and-place process using magnetic micro-gripper. Top section and bottom section of the video show top view and side view of the assembly process, respectively. All the hydrogels were sequentially manipulated individually using tele-operated control.

Video S3. Complex heterogeneous 3D assembly on eight different posts

This video shows heterogeneous 3D robotic assembly of various hydrogels on eight different posts. By repeating the robotic assembly with micro-gripper, various hydrogels were assembled up to three layers on eight different posts. Magnetic micro-gripper was capable of assembling complex heterogeneous systems by individually controlling not only the position of each hydrogel during assembly process, but also the type of the hydrogel and number of layers to get necessary heterogeneous 3D structure within enclosed aquatic environments.

[1] M. Ruths, J. N. Israelachvili. in *Springer Handbook of Nanotechnology* (ed Bharat Bhushan),Springer-Verlag Berlin Heidelberg, **2010**, Ch. 29.

[2] X. Shi, Y.-P. Zhao, *J. Adh. Sci. Tech.,* **2004**, *18*, 55-68.

Figure S1. Characterization of gripping. (a) Gripper in initial state. *L* and *w* are beam length and width, respectively. (b) In the hydrogel-holding state, the total beam deflection δ_{total} was defined as the distance between initial beam position and the deflected position due to holding hydrogel and affected by both the external magnetic torque *T* and the reactive normal force *N* from the hydrogel.

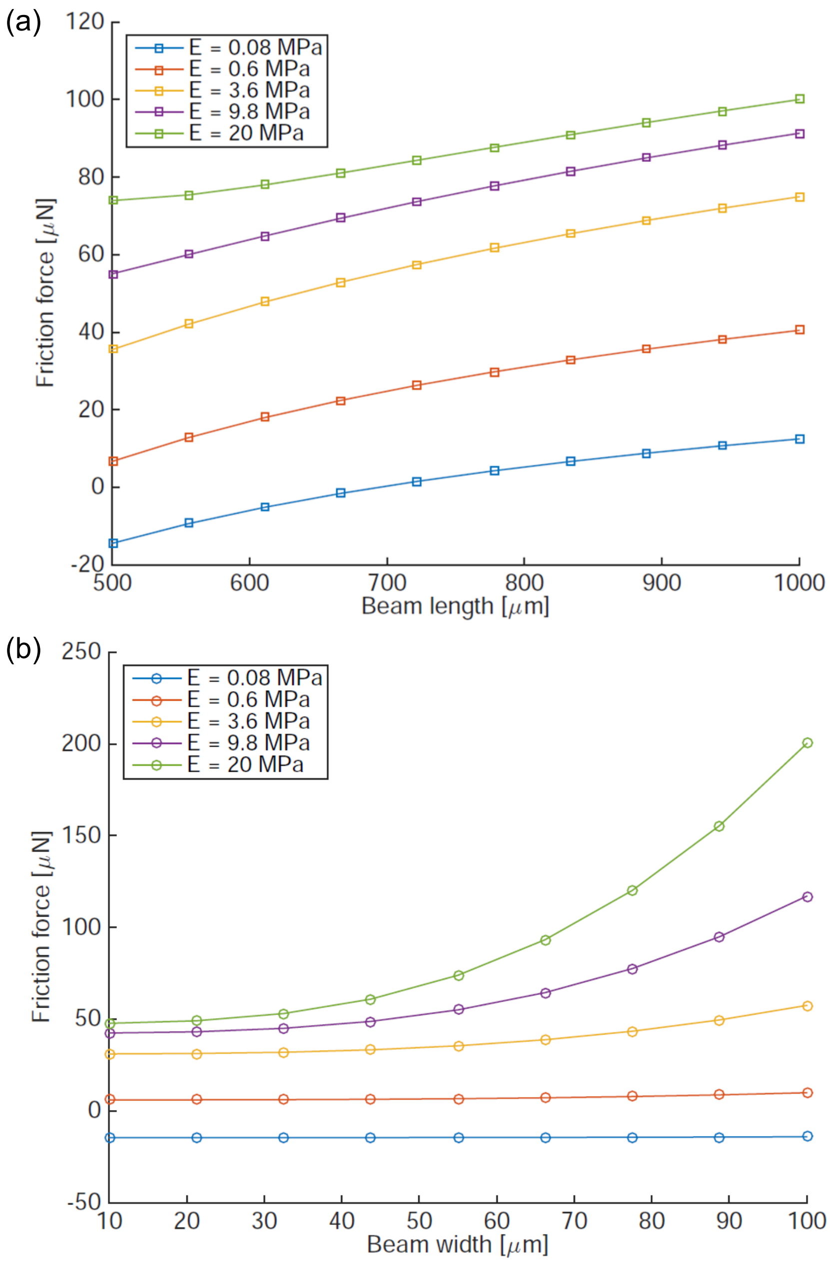

Figure S2. Simulation of the influence of (a) gripper beam length and (b) beam width under different material elastic modulus on the gripping friction force.

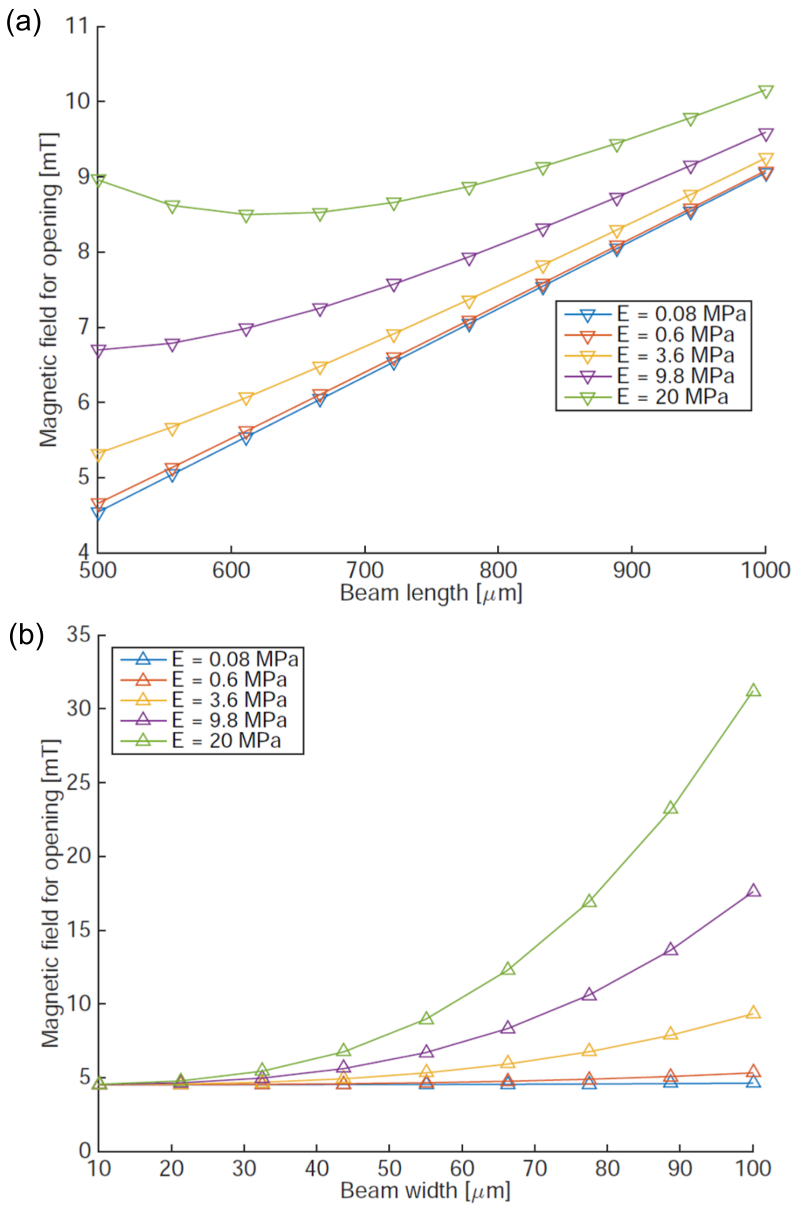

Figure S3. Simulation of the influence of (a) gripper beam length and (b) gripper beam width with different materials on the minimum required magnetic field for opening the micro-gripper tips.

Figure S4. Heterogeneous 3D robotic assembly of various hydrogels on four different posts. (a)-(e) Selected time-lapse images from a video of heterogeneous 3D assembly on multiple posts. (a) Micro-gripper gripped the first target hydrogel. (b) The hydrogel-holding gripper was levitated by applying magnetic gradient pulling force and moved to the target post. (c) The gripper moved downward and assembled the hydrogel on the post. (d)-(e) After repeated assembly of various hydrogels, the last hydrogel was aligned and assembled on the last target post. (f) Schematic illustration of heterogeneously assembled hydrogels on four different posts. Total twelve hydrogels with six different types were assembled up to three layers. Each code of hydrogel was represented as shape and color. (g)-(h) SEM images of heterogeneously assembled hydrogels on four different posts as illustrated in (f). White numbers on images correspond to the number of posts from (f). (g) Top image. (h) 3D view image. Scale bars, 1 mm. (i)-(k) Total eight hydrogels with seven different types were assembled on four posts up to three layers. (i) Illustrated schematic of the assembly. (j)-(k) Top and 3D view SEM images of (i), respectively. Scale bars, 1 mm.

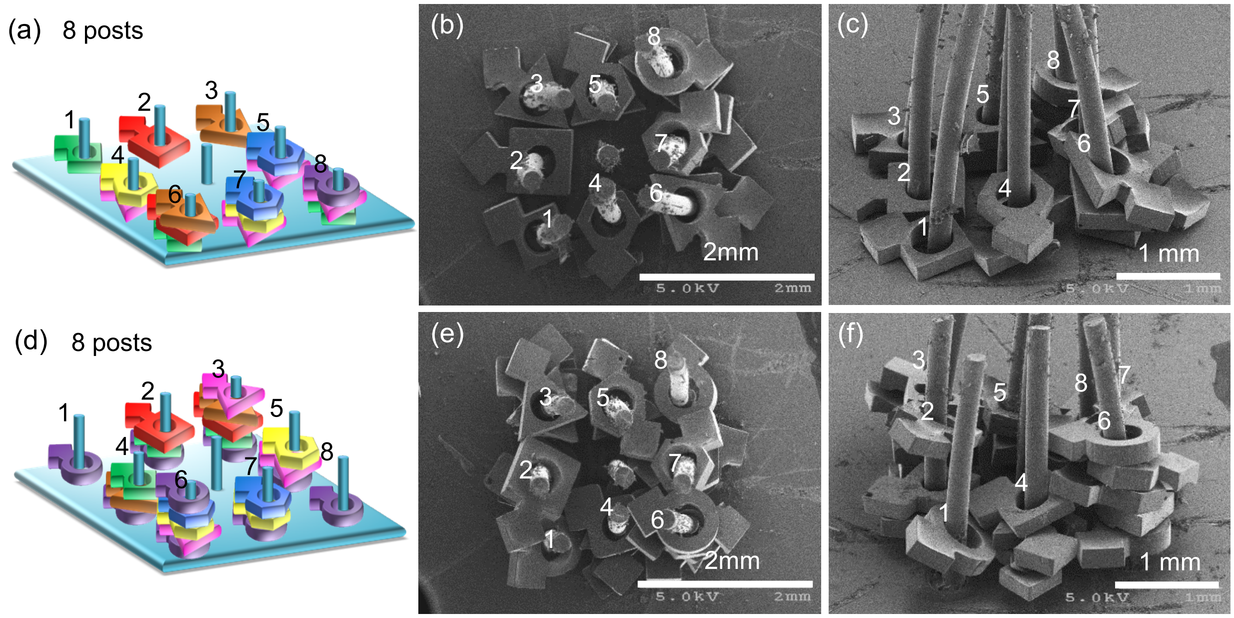

Figure S5. Complex heterogeneous 3D robotic assembly of various hydrogels on eight posts. (a) Schematic illustration of heterogeneously assembled hydrogels on eight different posts. Total fifteen hydrogels with seven different types were assembled on eight posts. (b)-(c) Top and 3D view SEM images of (a), respectively. (d)-(f) Total twenty-four hydrogels with seven different types were assembled on eight posts up to five layers. (d) Illustrated schematic of the assembly. (e)-(f) Top and 3D view SEM images of (i), respectively.